AMSR-E/Aqua Daily L3 6.25 km Sea Ice Drift Polar Grids, Version 1

USER GUIDE

How to Cite These Data

As a condition of using these data, you must include a citation:

Cavalieri, D. J., T. Markus, A. Ivanoff, A. K. Liu, and Y. Zhao. 2011. *AMSR-E/Aqua Daily L3 6.25 km Sea Ice Drift Polar Grids, Version 1*. [Indicate subset used]. Boulder, Colorado USA. NASA National Snow and Ice Data Center Distributed Active Archive Center. https://doi.org/10.5067/AMSR-E/AE_SID.001. [Date Accessed].

FOR QUESTIONS ABOUT THESE DATA, CONTACT NSIDC@NSIDC.ORG

FOR CURRENT INFORMATION, VISIT https://nsidc.org/data/AE_SID

National Snow and Ice Data Center

TABLE OF CONTENTS

1 DATA DESCRIPTION

1.1 Format

Data are stored in Hierarchical Data Format - Earth Observing System (HDF-EOS) format. Files contain core metadata, product-specific attributes, and the data fields in 4-byte floating point format. Missing data values are indicated by 0. Refer to Table 1 for parameter summary information.

Table 1. Parameter Summary Information

Field name	Description
SI_06km_NH_SEAICEDRIFT_SPD	Northern Hemisphere 5-day average speed (cm/s)
SI_06km_NH_SEAICEDRIFT_DIR	Northern Hemisphere 5-day average direction (radians)
SI_06km_SH_SEAICEDRIFT_SPD	Southern Hemisphere 5-day average speed (cm/s)
SI_06km_SH_SEAICEDRIFT_DIR	Southern Hemisphere 5-day average direction (radians)

1.2 File Naming Convention

This section explains the file naming convention used for this product with an example.

Example file name: AMSR_E_L3_SeaIceDrift_B01_20110630.hdf

AMSR_E_L3_SeaIceDrift_X##_yyyymmdd.hdf

Refer to Table 2 for the values of the file name variables listed above.

Table 2. Variable Values for the File Name

Variable	Description
X	Product Maturity Code (Refer to Table 3 for valid values.)
##	file version number
yyyy	four-digit year
mm	two-digit month
dd	two-digit day
hdf	Hierarchical Data Format (HDF)

Table 3. Variable Values for the Product Maturity Code

Variables	Description
P	Preliminary - refers to non-standard, near-real-time data available from NSIDC. These data are only available for a limited time until the corresponding standard product is ingested at NSIDC.
B	Beta - indicates a developing algorithm with updates anticipated.
T	Transitional - period between beta and validated where the product is past the beta stage, but not quite ready for validation. This is where the algorithm matures and stabilizes.
V	Validated - products are upgraded to Validated once the algorithm is verified by the algorithm team and validated by the validation teams. Validated products have an associated validation stage. Refer to Table 4 for a description of the stages.

Table 4. Validation Stages

Validation Stage	Description
Stage 1	Product accuracy is estimated using a small number of independent measurements obtained from selected locations, time periods, and ground-truth/field program efforts.
Stage 2	Product accuracy is assessed over a widely distributed set of locations and time periods via several ground-truth and validation efforts.
Stage 3	Product accuracy is assessed, and the uncertainties in the product are well-established via independent measurements made in a systematic and statistically robust way that represents global conditions.

Table 5 provides examples of file name extensions for related files that further describe or supplement data files.

Table 5. Related File Extensions and Descriptions

Extensions for Related Files	Description
.jpg	Browse data
.qa	Quality assurance information
.ph	Product history data
.xml	Metadata files

1.3 File Size

Each daily granule is approximately 30 MB.

1.4 Spatial Coverage

1.4.1 Spatial Coverage Map

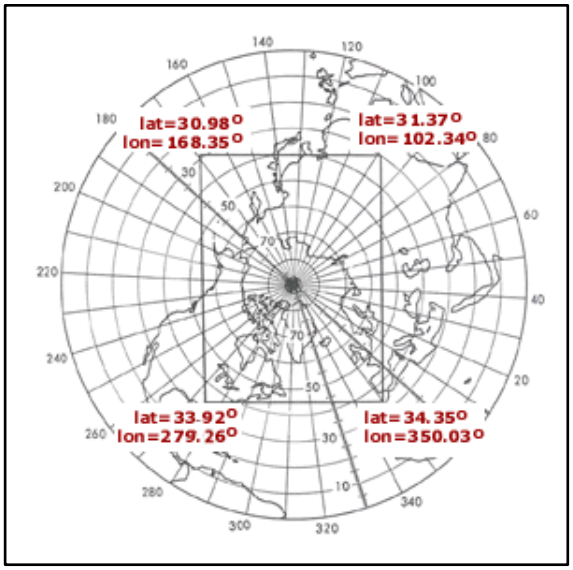

Figure 1. Northern Hemisphere

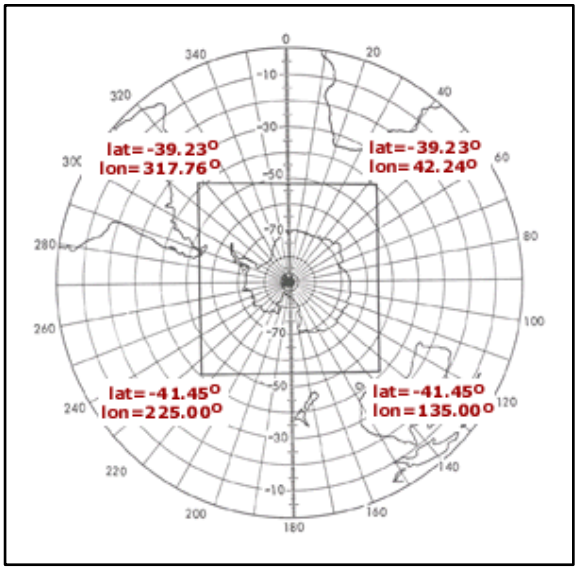

Figure 2. Southern Hemisphere

1.4.2 Spatial Resolution

Spatial resolution is 6.25 km for the north and south polar projections. Data points are spaced every 100 km, or every 16th grid point.

1.4.3 Projection

Sea ice drift grids are in a polar stereographic projection, which specifies a projection plane such as the grid, tangent to the earth at 70 degrees. The planar grid is designed so that the grid cells at 70 degrees latitude are 6.25 km by 6.25 km. For more information on this topic please refer to (Pearson 1990) and (Snyder 1987).

Polar stereographic projections often assume that the plane (grid) is tangent to the Earth at the pole, such that there is a one-to-one mapping between the Earth's surface and grid and no distortion at the pole. As such, distortion in the grid increases as latitude decreases (because more of the Earth's surface falls into any given grid cell), to a maximum of 31% at the edge of the northern polar grid and 22% at the edge of the southern polar grid.

The NSIDC Polar Stereographic Projection is true at 70 degrees rather than the poles to minimize distortion at the ice margins. This increases the distortion at the poles by 3% and decreases the

distortion at the grid edges by the same amount. It also reduces the total number of grid cells in each grid as the Earth's surface is more accurately represented.

The polar stereographic formulas for converting between latitude/longitude and X-Y grid coordinates are taken from Snyder (1982). This projection assumes a Hughes ellipsoid with a radius of 3443.992 nautical mi or 6378.273 km and an eccentricity (e) of 0.081816153 (or e2 = 0.006693883). The structural metadata (StructMetadata.0) built into the HDF-EOS data file lists the squared eccentricity value rounded to four significant digits (0.006694).

1.4.4 Grid Description

Northern Hemisphere: 1216 columns by 1792 rows
Southern Hemisphere: 1264 columns by 1328 rows

The approximate outer boundaries of the grids are defined in Tables 6 and 7. Corner points are listed starting from the upper left and reading clockwise. Interim rows define boundary midpoints.

Table 6. North Polar Grid

X (km)	Y (km)	Latitude (deg)	Longitude (deg)	Pixel Location
-3850	5850	30.98	168.35	corner
0	5850	39.43	135.00	midpoint
3750	5850	31.37	102.34	corner
3750	0	56.35	45.00	midpoint
3750	-5350	34.35	350.03	corner
0	-5350	43.28	315.00	midpoint
-3850	-5350	33.92	279.26	corner
-3850	0	55.50	225.00	midpoint

Table 7. South Polar Grid

X(km)	Y(km)	Latitude (deg)	Longitude (deg)	Pixel Location
-3950	4350	-39.23	317.76	corner
0	4350	-51.32	0.00	midpoint
3950	4350	-39.23	42.24	corner
3950	0	-54.66	90.00	midpoint
3950	-3950	-41.45	135.00	corner
0	-3950	-54.66	180.00	midpoint
-3950	-3950	-41.45	225.00	corner
-3950	0	-54.66	270.00	midpoint

For this product, there are tar files that contain geolocation and pixel-area tools, which provide the same functionality for all polar stereographic passive microwave sea ice data sets at NSIDC. These tools include a FORTRAN routine called locate, a latitude/longitude grid, and a pixel-area grid.

The geocoordinate FORTRAN tools available are the following. They are available via HTTPS.

- **locate.for**: A FORTRAN routine that allows the user to enter an i,j coordinate and get the corresponding latitude/longitude coordinate, and vice versa.
- **mapll.for** and **mapxy.for**: Subroutines that are associated with the locate.for program. These programs need to be compiled, but are not run explicitly. They are called by locate.for. Thus, the user should compile these programs with locate.for and then use locate to do the conversions.

The latitude/longitude grids are in binary format and are stored as long word integers (4 byte) scaled by 100,000. Each array location (i,j) contains the latitude or longitude value at the center of the corresponding data grid cells. These tar files are available via FTP.

Table 8. Tar Files Variable Description

Variables Used in Tar Files	Description
pss	polar stereographic southern projection
psn	polar stereographic northern projection
06, 12, & 25	6 km, 12 km, & 25 km
lat	latitude grid
lon	longitude grid
area	pixel area

1.5 Temporal Coverage

See the AMSR-E Data Versions Web page for a summary of temporal coverage for different AMSR-E products and algorithms.

1.5.1 Temporal Resolution

Daily sea ice drift values are produced using a five-day window. Thus, the resulting speed and direction for a given day represent an average displacement velocity over five days. The file AMSR_E_L3_SeaIceDrift_B01_20110630.hdf, for example, contains the five-day average velocity from 28 June to 02 July 2011.

1.6 Parameter or Variable

Refer to the Table 1 in the Format section of this document for a list of parameters used in this data set.

1.6.1 Parameter Description

The parameters of this data set include sea ice speed (cm/s) and sea ice direction (radians). The range for direction is +pi to -pi radians. Thus, from the horizontal axis of the middle of the image, values in the counterclockwise direction are 0 to +pi, and values in the clockwise direction are -pi to 0.

2 DATA ACQUISITION AND PROCESSING

2.1 Theory of Measurements

Sea ice drift products are used to understand the circulation regimes and patterns of sea ice, and for time analyses and process studies in the Arctic and Antarctic. As stated by Zhao and Liu (2007), sea ice motion not only influences sea-ice mass balance as it is displaced and redistributed, but it also plays a role in the redistribution of latent and sensible heat flux. Less ice cover and/or thinner ice results in more heat exchange between the ocean and the atmosphere, whereas more ice cover and/or thicker ice results in less heat exchange. Yet even since the advent of the satellite era in the 1970s, obtaining reliable sea ice drift measurements has proved difficult due to factors such as cloud cover, low-light levels, and the dynamic nature of sea ice, particularly along coastlines, the marginal ice zone, or during the summer months—all of which result in less contrast between sea ice and the open ocean (Liu and Cavalieri 1998).

Passive microwave data, however, are particularly useful for sea ice studies due to the relatively high contrast in emissivities between open water and sea ice. The satellite-received radiation, expressed as a brightness temperature, is discussed by Cavalieri and Comiso (2000). Furthermore, due to its higher spatial resolution (6.25 km) and daily temporal coverage, the 89 GHz channel of the AMSR-E passive microwave radiometer is especially useful for sea ice studies. Thus, to calculate sea ice drift, which includes sea ice speed and direction, an algorithm called the wavelet transform is applied to the 89 GHz passive microwave brightness temperatures from AMSR-E as a basis for time-varying signal analysis (Liu and Cavalieri 1998). According to Zhao and Liu (2003), the use of this algorithm results in more detail and smoother sea ice motion in the fall, winter, and spring months and also permits the derivation of sea ice motion during the summer months when sea ice features change rapidly due to melting and ponding and are therefore difficult to track.

2.2 Derivation Techniques and Algorithms

2.2.1 Sea Ice Drift

This sea ice drift product is generated using the wavelet transform algorithm developed at Goddard Space Flight Center (GSFC) and described by Liu and Cavalieri (1998). Wavelet transform sea ice speed and direction are derived for both the Arctic and the Antarctic using gridded and averaged AMSR-E brightness temperatures.

To determine drift vectors only over sea ice, not open water, a sea ice mask is used within the sea ice drift algorithm code. Derived from the 18 GHz and 37 GHz Vertical (V) channels of the AMSR-E L3 12.5 km brightness temperature product, the mask approximates sea ice coverage in order to mask out unused vector points.

The following has been adapted from Liu and Cavalieri (1998) and describes the derivation techniques:

The wavelet transforms of satellite images can be used for near-real-time quick-look analyses of satellite data for feature detection, for data reduction using a binary image, and image enhancement by edge linking. In general, the continuous wavelet transform, Ws (a, b), of a function, s (r), where r = (x, y), is expressed in terms of the complex valued wavelet function, w(r), as follows:

$$W_S(a, \boldsymbol{b}) = \frac{1}{\sqrt{a}} \int s(\boldsymbol{r}) w^* \left(\frac{\boldsymbol{r}-\boldsymbol{b}}{a} \right) d\boldsymbol{r} \qquad \text{(Equation 1)}$$

in which the wavelet function is dilated by a factor a, and shifted by b. The function w(r) is the basic wavelet (Combes et al. 1989). The superscript * indicates complex conjugate. For data analysis, the wavelets frequently used are: a Gaussian modulated sine and cosine wave packet, known as the Morlet wavelet; and the second derivative of a Gaussian, often referred to as the Mexican hat.

- Closed contours (those with no other features crossing them, called zero-crossing contours) correspond to the boundary of ice features. Yet these zero-crossing contours may contain many different ice features. To associate a single closed contour with an isolated ice feature, a five percent threshold above the minimum of the wavelet transform is applied as the contour value.
- Next, each closed contour is framed in a rectangular window with its four sides just tangent to the four extreme locations of the closed contour. Each window at a given starting date is used as a template to be matched. The template window is not fixed in size, but is determined by the ice feature at a particular location.
- With the template defined, the templates are then matched with the results from the wavelet transform of the AMSR-E image four days later. Because of the 6.25 km resolution of the AMSR-E image, the displacement of the ice feature may move just a pixel or two in

several days. Thus, the domain of the template matching can be restricted to an area with a few pixels (such as 20 pixels) larger than the template window. The matching is done by shifting the template over each pixel in the domain.

- For each location, the absolute values of the differences between the shifted template values and the target values are then summed.
- The sequence of the summation values is then used as a metric of the degree of match of the ice feature. Its minimum indicates a possible match of two displaced ice features. Once the shapes have been matched, the velocity vector can be easily estimated from dividing the relative displacement over a time interval of four days.

Note that the method of template matching outlined above uses a template window determined by the threshold of the wavelet transform of AMSR-E images. This method of template matching of ice features is very efficient, as the only computations involved are logical operations, addition, and subtraction. Furthermore, it is only necessary to match the template pattern to a limited number of target patterns generated by the results of the wavelet transform, not to every location in the image as with classical template matching. Note also that although template correlation is applied here only to find the translation of the target pattern with respect to the template pattern, it can be extended to find the rotation of the target pattern by incremental rotation of the target pattern in direction and then matching the extent of their agreement (Liu and Cavalieri 1998).

Using the resulting wavelet transform distance, speed is then determined by averaging the sea ice distance over five days, for example:

$$\frac{d2 - d1}{t2 - t1}$$

where:

d = distance
t = time

Speed is given as the magnitude of motion in centimeters per second (cm/s). Direction is determined by calculating radians from the horizontal axis of the grid counterclockwise.

2.2.2 Processing Steps

These data were processed at the AMSR-E GHCC-SIPS, the Global Hydrology and Climate Center Science Investigator-led Processing System, and were derived by applying the GSFC sea ice drift algorithm to AMSR-E brightness temperatures. Sea ice speed and direction were determined using the 89 GHz Horizontal (H) channel of the AMSR-E/Aqua Daily L3 6.25 km 89 GHz Brightness Temperature Polar Grids product, and the sea ice mask used in the drift algorithm code was derived from the 18 GHz and 37 GHz Vertical (V) channels of the AMSR-E/Aqua Daily L3 12.5 km

Brightness Temperature, Sea Ice Concentration, & Snow Depth Polar Grids product.
For more information, refer to the Derivation Techniques and Algorithms section to this document.

2.2.3 Processing History

See AMSR-E Data Versions for a summary of algorithm changes since the start of mission.

2.2.4 Error Sources

See the AMSR-E/Aqua L2A Global Swath Spatially-Resampled Brightness Temperatures guide document for information about potential errors with constructed brightness temperatures.

With regards to the wavelet transform algorithm, a comparison of the AMSR-E sea ice drift retrievals with Arctic Ocean buoys results in a Root-Mean-Square (RMS) ice speed error of 3 cm/s and an RMS direction error of 26 degrees (Zhao and Liu 2007).

2.3 Sensor or Instrument Description

Please refer to the AMSR-E Instrument Description document.

2.4 Quality Assessment

Each HDF-EOS file contains core metadata with Quality Assessment (QA) metadata flags that are set by the Science Investigator-led Processing System (SIPS) at the Global Hydrology and Climate Center (GHCC) prior to delivery to NSIDC. A separate metadata file in XML format is also delivered to NSIDC with the HDF-EOS file; it contains the same information as the core metadata. Three levels of QA are conducted with the AMSR-E Level-2 and -3 products: automatic, operational, and science QA. If a product does not fail QA, it is ready to be used for higher-level processing, browse generation, active science QA, archive, and distribution. If a granule fails QA, SIPS does not send the granule to NSIDC until it is reprocessed. Level-3 products that fail QA are never delivered to NSIDC (Conway 2002).

2.4.1 Automatic QA

Weather filters are employed for the Level-3 sea ice products to eliminate spurious sea ice concentrations over open ocean resulting from varying atmospheric emission. The weather filters are based on threshold values for the spectral gradient ratio and thresholds derived from brightness temperature differences. Sea ice products are checked to see if ice concentration values fall within reasonable limits. These limits are based in part on satellite sea ice climatology developed since the Scanning Multichannel Microwave Radiometer (SMMR) era in 1978.

2.4.2 Operational QA

AMSR-E Level-2A data arriving at GHCC are subject to operational QA prior to processing higher-level products. Operational QA varies by product, but it typically checks for the following criteria in a given file (Conway 2002):

- File is correctly named and sized
- File contains all expected elements
- File is in the expected format
- Required EOS fields of Time, Latitude, and Longitude are present and populated
- Structural metadata is correct and complete
- The file is not a duplicate
- The HDF-EOS version number is provided in the global attributes
- The correct number of input files were available and processed

2.4.3 Science QA

AMSR-E Level-2A data arriving at GHCC are also subject to science QA prior to processing higher-level products. If less than 50 percent of a granule's data is good, the science QA flag is marked suspect when the granule is delivered to NSIDC. In the SIPS environment, the science QA includes checking the maximum and minimum variable values, and percent of missing data and out-of-bounds data per variable value. At the Science Computing Facility (SCF), also at GHCC, science QA involves reviewing the operational QA files, generating browse images, and performing the following additional automated QA procedures (Conway 2002):

- Historical data comparisons
- Detection of errors in geolocation
- Verification of calibration data
- Trends in calibration data
- Detection of large scatter among data points that should be consistent

Geolocation errors are corrected during Level-2A processing to prevent processing anomalies such as extended execution times and large percentages of out-of-bounds data in the products derived from Level-2A data.

The Team Lead SIPS (TLSIPS) developed tools for use at SIPS and SCF for inspecting the data granules. These tools generate a QA browse image in Portable Network Graphics (PNG) format and a QA summary report in text format for each data granule. Each browse file shows Level-2A and Level-2B data. These are forwarded from RSS to GHCC along with associated granule information, where they are converted to HDF raster images prior to delivery to NSIDC.

Please refer to AMSR-E Validation Data for information about data used to check the accuracy and precision of AMSR-E observations.

3 REFERENCES AND RELATED PUBLICATIONS

Cavalieri, D. and J. Comiso. 2000. Algorithm Theoretical Basis Document for the AMSR-E Sea Ice Algorithm, Revised December 1. Landover, Maryland USA: Goddard Space Flight Center.

Combes, J. M., A. Grossmann, and P. Tchamitchian. 1989. Wavelet: Time Frequency Methods and Phase Space. Proceedings of the International Conference on Wavelet, Marseille, France. *New York: Springer-Verlag*. 331.

Conway, D. 2002. Advanced Microwave Scanning Radiometer - EOS Quality Assurance Plan. Huntsville, Alabama USA: Global Hydrology and Climate Center.

Liu, A. K. and D. J. Cavalieri. 1998. On Sea Ice Drift from the Wavelet Analysis of the Defense Meteorological Satellite Program (DMSP) Special Sensor Microwave Imager (SSM/I) Data. *International Journal of Remote Sensing* 19:7, 1415-1423. doi: 10.1080/014311698215522

Pearson, F. 1990. *Map Projections: Theory and Applications*. CRC Press. Boca Raton, Florida USA. 372 pages.

Snyder, J.P. 1987. *Map Projections - A Working Manual*. U.S. Geological Survey Professional Paper 1395. U.S. Government Printing Office. Washington, D.C. USA. 383 pages.

Snyder, J. P. 1982. *Map Projections Used by the U.S. Geological Survey*. U.S. Geological Survey Bulletin 1532.

Zhao, Y. and A. K. Liu. 2007. Arctic Sea-Ice Motion and Its Relation to Pressure Field. *Journal of Oceanography* 63:505-515.

Zhao, Y. and A. K. Liu. 2003. Applications of Sea Ice Motion and Deformation Derived from Satellite Data. p. 238-248. Proceedings of SPIE, 5155, ed. by R. J. Frouin, G. D. Gilbert and D. Pan, SPIE, Bellingham, Washington USA. doi: http://dx.doi.org/10.1117/12.504764

Zhao, Y. and A. K. Liu. 2001. Principal-Component Analysis of Sea Ice Motion from Satellite Data. *Ann. Glaciol.*, 33, 133-138.

For more information regarding related publications, see the Research Using AMSR-E Data Web page.

4 CONTACTS AND ACKNOWLEDGMENTS

4.1 Investigator(s) Name and Title

Donald J. Cavalieri and **Thorsten Markus**
Hydrospheric and Biospheric Sciences Laboratory

5 DOCUMENT INFORMATION

5.1 Publication Date

April 2011

5.2 Date Last Updated

23 April 2021